



Deformation Behavior of X70 Pipeline Steel Under Hot Straightening Condition

Zhanyuan Xue¹, Ben Guan^{1,2}(✉), and Yong Zang^{1,2}

¹ School of Mechanical Engineering, University of Science and Technology Beijing, Beijing, China

niuben57@163.com

² Shunde Graduate School, University of Science and Technology Beijing, Beijing, Guangdong, China

Abstract. During the hot straightening process, the sheet undergoes multiple tensile and compressive deformation cycles. In this paper, cyclic tensile tests and microstructure observation under different strain amplitude, temperature, and strain rates were carried out. The macroscopic deformation behavior and microstructure evolution of X70 pipeline steel under cyclic tension and compression load were investigated, then, macroscopic mechanical properties and microstructure evolution of sheet steel in the process of hot straightening were deeply understood. The experimental results show that the X70 pipeline steel has the characteristics of cyclic hardening. Compared with temperature and strain rate, the hysteresis loop was dominantly influenced by strain amplitude. There is little difference between the peak value and the trough value of the circulating stress in the hysteresis loop. Hot straightening has little effect on the microstructure of the material. The study shows that the amount of deformation has a great influence on the deformation behavior of materials during the process of hot straightening, and the Bauschinger effect of materials is not obvious. The material deformation in the process of hot straightening belongs to the macroscopic deformation behavior.

Keywords: Cyclic tension-compression · Cyclic hardening · Hot straightening

1 Introduction

X70 is a type of pipeline steel that is commonly used in the oil and gas industry for the construction of pipelines. This type of steel is known for its high strength and toughness, making it well-suited for use in harsh, high-stress environments. X70 steel is typically made through a combination of casting and rolling processes, followed by heat treatment to improve its mechanical properties. The chemical composition of X70 pipeline steel typically includes low carbon content, high levels of manganese, and small amounts of other elements such as vanadium, niobium, and titanium. Vanadium mainly serves as a precipitation strengthening phase that precipitates at low temperatures in needle-like ferrite to increase the strength of the steel. Vanadium carbide formed with carbon can improve the corrosion resistance of the steel under high-temperature and high-pressure

conditions. Niobium is beneficial for increasing the phase transformation fraction of austenite during the phase transformation of ferrite after de-formation. Titanium mainly acts as a fine crystal reinforcement and precipitation strengthening agent, which can increase the strength and toughness of the steel. These elements work together to provide the necessary combination of strength, toughness, and corrosion resistance for pipeline applications [1, 2].

The hot straightening process is typically viewed as a preliminary step in controlling geometric defects during plate production. However, the high strength of X70 tubular steel makes it challenging to eliminate defects in subsequent cold working processes after controlled rolling and cooling. As the last heat deformation process in the medium-thick plate production line, the hot straightening process requires detailed examination. The root cause of plate geometric defects is the uneven distribution of stress. In the hot straightening process, X70 pipeline steel undergoes multiple reciprocals bending deformations under high temperatures. The macro-mechanical properties and post-correction microstructure of the X70 pipeline steel plate are related to subsequent processing and forming. Therefore, it is essential to study the stress-strain state of reciprocal bending and post-correction microstructure evolution during the hot straightening process. Previous studies on thermal straightening have primarily focused on the evolution of plate curvature, bending moment, residual stress, and other parameters [3–7]. However, further research is required to understand the cyclic deformation characteristics of hot straightening fully.

Therefore, this paper investigates the macroscopic performance and microstructure evolution of X70 pipeline steel under different thermal deformation conditions of high-temperature cyclic tensile loading. To do this, high-temperature cyclic tensile tests and subsequent microstructure observations were carried out based on the thermal deformation conditions of X70 pipeline steel for hot straightening. The aim is to gain an understanding of the mechanical property evolution law of hot straightening.

2 Material and Experimental Procedure

2.1 Materials

The test material is a hot-rolled X70 pipeline steel plate with a thickness of 18mm, annealed state, and its chemical composition is shown in Table 1.

Table 1. Chemical composition of X70 steel sheet (wt%).

C	Si	Mn	V	Ti	Nb	P	S
0.16	0.45	1.7	0.06	0.06	0.05	0.02	0.01

2.2 High-Temperature Cyclic Tensile Test

The high-temperature cyclic tensile testing of X70 pipeline steel was carried out using the MTS-370.10 fatigue tester, as illustrated in Fig. 1(a). A 12-mm scale quartz rod contact high-temperature strain gauge was utilized for measuring the strain.

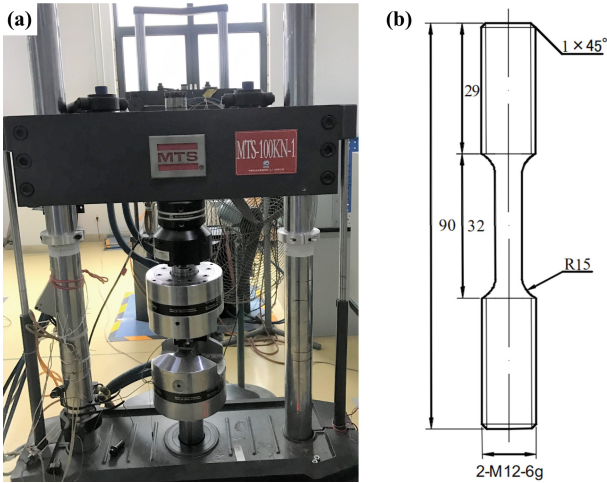


Fig.1. High-temperature cyclic tensile testing equipment and specimens.

The geometry and size of the specimens were determined according to the test standard GB/T 15248-2008 and the specifications of the testing machine, as illustrated in Fig. 1(b). The test material was divided into samples using CNC programmed wire cutting equipment, with the length direction of the specimen matching that of the test material steel plate rolling. To ensure the absence of scratches, damage, or rust on the surface of the working section, the latter was finely processed through longitudinal polishing before testing.

2.3 High-Temperature Cyclic Tensile Test Parameters and Scheme

The parameters to be determined for the high-temperature cyclic tensile test include the deformation temperature T , the strain amplitude $\Delta\varepsilon/2$, and the strain rate $\dot{\varepsilon}$, which are determined as shown below.

- 1) Deformation temperature T : The appropriate straightening temperature can promote some changes in the tissue structure of the board, thereby enhancing its plasticity and deformation ability. As the temperature increases, the lattice structure in the board changes, causing the originally tightly arranged grains to become loose, and the crystals contain many dislocations, thus exhibiting higher plasticity and smaller rebound. This temperature can also make the stress distribution in the board more uniform, thereby reducing distortion and deformation during the deformation process. According to the X70 pipeline steel hot straightening process [8], it is known that the hot straightening temperature range of X70 pipeline steel after controlled cooling is 350 °C to 550 °C, i.e., the experimental deformation temperature is determined.
- 2) Strain amplitude $\Delta\varepsilon/2$: According to the analytical model of press bending in the roll-type hot straightening process for medium-thick plates [9], the multi-roll straightening machine first determines the maximum plastic deformation rate or maximum total deformation curvature that the plate can achieve when determining the amount of

press bending of the straightening rolls. For example, in the 11-roller hot straightening machine with the upper row of 5 rolls and the lower row of 6 rolls, the first and last rolls of the lower row of the roll system are adjusted individually for the amount of bending, and the other rolls are adjusted as a whole, and the maximum amount of bending is at the third roll, i.e., the third roll is the location of the maximum deformation of the plate, and the amount of bending and the corresponding strain is calculated as shown in Eq. (1), and the relationship between the curvature and the amount of bending is shown in Fig. 2(a). According to the reciprocal bending uniform curvature theorem [10], it is known that the tensile deformation and compressive deformation of hot straightening at the same cross-sectional position are equal. Based on Eq. (1), the maximum strain value of $\pm 1.0\%$ for the high-temperature cyclic drawing test was determined by combining the actual inlet and outlet bending of X70 pipeline steel in the temperature range of $350\text{ }^{\circ}\text{C}$ to $550\text{ }^{\circ}\text{C}$ and the corresponding hot straightening at a thickness of 18 mm as shown in Table 2 [9]. According to the standard GB T709-2019 corresponding to the unevenness of X70 pipeline steel, the minimum strain amplitude of the high-temperature cyclic drawing test was determined to be $\pm 0.5\%$, i.e., the strain amplitude range of the high-temperature cyclic drawing test was $\pm 0.5\%$ to $\pm 1.0\%$.

$$\begin{cases} \delta_i = \frac{\delta_2 - \delta_{10}}{4} t (i = 4, 6, 8, t = 3, 2, 1) \\ \delta_j = \frac{\delta_{j-1} + \delta_{j+1}}{2} (j = 3, 5, 7, 9) \\ \delta_3 = \frac{\delta_2 + \delta_4}{2} \\ \delta_4 = \frac{3}{4}\delta_2 + \frac{1}{4}\delta_{10} \\ r_3^2 = (r_3 - \delta_3)^2 + \left(\frac{l}{4}\right)^2 \\ \varepsilon_3 = \frac{h}{2r_3} \end{cases} \quad (1)$$

In Eq. (1), δ_i represents the upper row of straightening rollers, t is the decreasing ratio of the overall tilt adjustment of the upper row of straightening rollers as shown in Fig. 2(b), δ_j represents the lower row of straightening rollers, r_3 is the radius of the reverse bending rate of the third roll, l is the distance between adjacent straightening rollers on the horizontal line, h is the thickness of the cross-section of the straightened sheet, and ε_3 is the strain of the sheet at the third roll.

Table 2. Straightening parameters of the 11-roller hot straightening machine.

Materials	Thickness	Roll distance	Straightening speed	Deformation speed	Inlet/outlet bending
X70	18 mm	300 mm	0–500 mm/s	0–10 mm/s	3.58/0 mm

3) Strain rate $\dot{\varepsilon}$: Roll straightening is a planar strain state of reciprocal tensile-compressive strain along the normal direction of the sheet being straightened. Therefore, its strain and strain rate are equivalent. The strain rate in the hot straightening process of medium-thick plate has a gradient in the plate cross-section, assuming that the plate

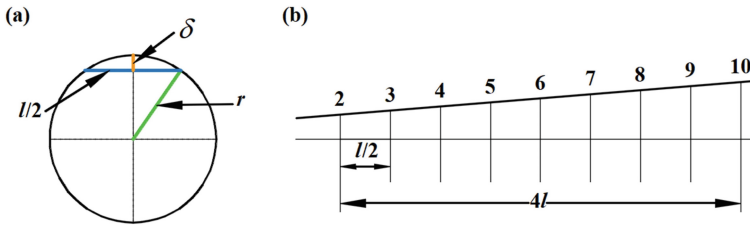


Fig. 2. Bending volume distribution between the radius of curvature calculation and roll 2 to roll 10.

is in point contact with the straightening rollers, the middle point of the upper and lower straightening rollers is the zero bending moment point, and the maximum bending moment point is in the contact position between the straightening rollers and the plate, as shown in Fig. 3. The time required from the zero moment point to the maximum bending moment point $t = \frac{L}{4v}$, so the strain rate $\dot{\epsilon}$ in the plate cross-section during the hot straightening process of the thick plate is distributed as shown in Eq. (2) below. According to the straightening parameters in Table 2, the strain rate range for the hot straightening process was obtained from 0 to 0.06 s^{-1} , but the strain rate range for the experiment was set to 0.0005 s^{-1} to 0.05 s^{-1} due to the equipment conditions of the high-temperature cyclic tensile testing machine.

$$\begin{cases} \dot{\epsilon} = \frac{\epsilon}{t} \\ t = \frac{L}{4v} \\ \dot{\epsilon} = \frac{4\epsilon v}{L} \end{cases} \quad (2)$$

In Eq. (2), ϵ is the strain, $\dot{\epsilon}$ is the strain rate, v is the straightening speed, and L indicates the spacing between adjacent straightening rolls on the horizontal line.

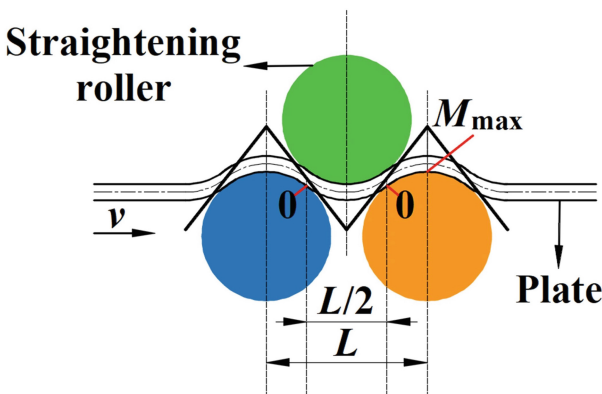


Fig. 3. Distribution of straightening roll bending moment under ideal conditions.

The high-temperature cyclic tensile test was performed in strain-controlled low perimeter symmetric control mode, and the test protocols for different heat deformation parameters are shown in Table 3. The tests were divided into three groups according to the type of thermal deformation parameters, and only one parameter was changed in each group, and the values of other parameters were unchanged. The magnitude of the corresponding thermal deformation conditions is determined based on the above range of thermal deformation parameters.

Table 3. High-temperature cyclic tensile test scheme.

Temperature (°C)	strain rate (s^{-1})	strain amplitude (%)	strain ratio	cycle number
450	0.005	0.5/0.75/1.0	-1	10
350/450/550	0.005	0.75	-1	10
450	0.0005/0.005/0.05	0.75	-1	10

2.4 Microstructure Experiments

To investigate the influence of temperature and strain rate on the microstructure of X70 pipeline steel during the hot straightening process, the specimens were examined using a JSM-7200F field emission scanning electron microscope and the orientation imaging analysis was conducted using an HKL EBSD Channel 5 system both before and after the high-temperature cyclic drawing test. As depicted in Fig. 4(a), the microstructure before the high-temperature cyclic drawing test exhibits a jagged or wavy morphology with uneven size, and the material organization demonstrates quasi-polygonal ferrite with a significant distribution of grain boundary orientation difference merit. Grain boundary analysis, shown in Fig. 4(b), reveals that ferrite grains contained a high-angle grain boundary (red) and more substructure with low angle grain boundary (black).

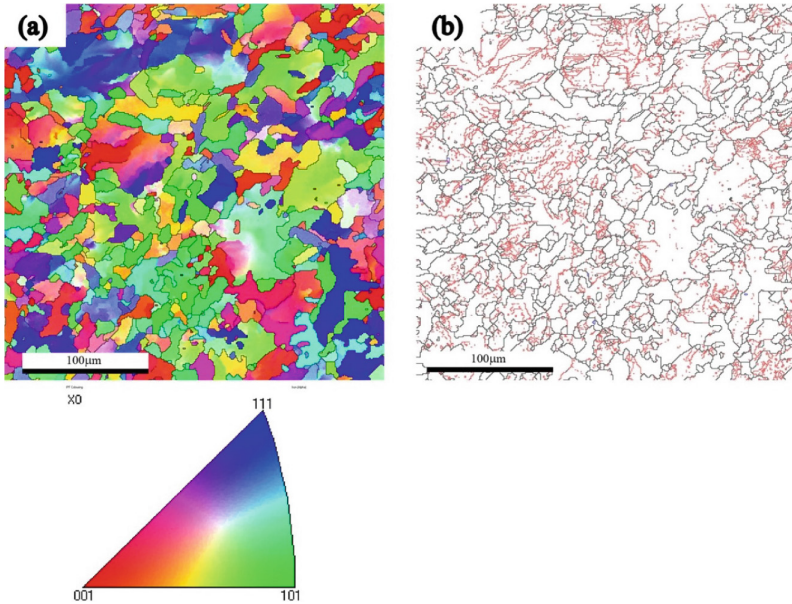


Fig.4. Microstructure of original specimen: (a) Grain distribution, (b) Distribution of grain boundaries.

3 Results and Discussion

3.1 Stress-Strain Response of X70 Pipeline Steel Under High-Temperature Cyclic Tensile Loading Conditions

The hysteresis curves and cyclic stress amplitudes resulting from high-temperature cyclic tensile loading under different heat deformation conditions are presented in Figs. 5–8.

The analysis of Figs. 5 through 7 reveals a small difference between the upper and lower portions of the hysteresis curve envelope for each weekly cycle of X70 pipeline steel, indicating that the material's Bauschinger effect is not significant. Figure 8 shows that X70 pipeline steel experiences rapid cyclic hardening at the beginning of the cycle, as the stress amplitude reaches its maximum value in under four weekly cycles and enters a stress steady state.

Figures 5 and 7 show that the cyclic stress amplitude of X70 pipeline steel gradually increases with the number of cycles, and the height of the stress-strain hysteresis loop increases with the strain amplitude or strain rate. This indicates a positive correlation between the stress-strain response of X70 pipeline steel in the initial cycle and the strain amplitude or strain rate. In contrast, Fig. 6 reveals that the height of the stress-strain hysteresis loop decreases as the temperature increases, suggesting a negative correlation between the stress-strain response of the initial cycle of X70 pipeline steel and temperature.

By comparing the distribution of cyclic stress amplitude under different thermal deformation conditions in Fig. 8, it is evident that the strain and temperature can exert

a greater influence on the cyclic deformation of the material within the corresponding thermal deformation condition range.

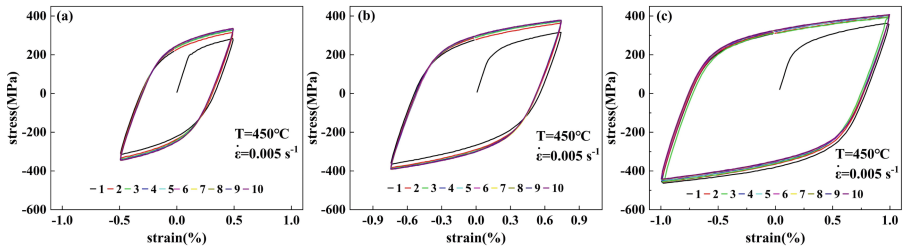


Fig. 5. Hysteresis curves of high-temperature cyclic tensile loads at different strain amplitudes: (a) $\Delta\varepsilon/2 = 0.5\%$, (b) $\Delta\varepsilon/2 = 0.75\%$, (c) $\Delta\varepsilon/2 = 1.0\%$.

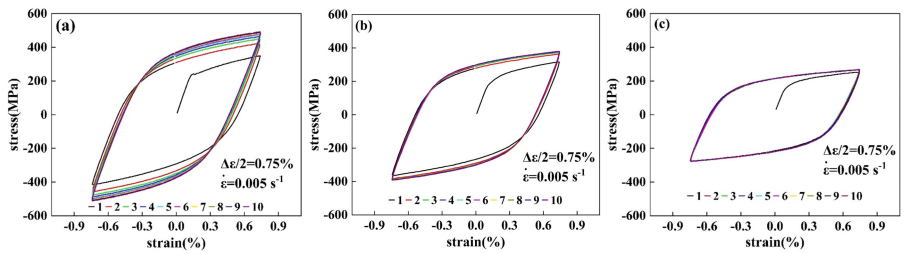


Fig. 6. Hysteresis curves of high-temperature cyclic tension-compression loads at different temperatures: (a) $T = 350\text{ }^{\circ}\text{C}$, (b) $T = 450\text{ }^{\circ}\text{C}$, (c) $T = 550\text{ }^{\circ}\text{C}$.

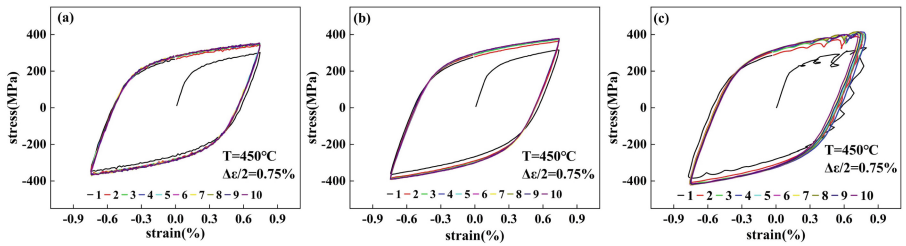


Fig. 7. Hysteresis curves of high-temperature cyclic tension-compression loads at different strain rates: (a) $\dot{\varepsilon} = 0.0005\text{ s}^{-1}$, (b) $\dot{\varepsilon} = 0.005\text{ s}^{-1}$, (c) $\dot{\varepsilon} = 0.05\text{ s}^{-1}$.

3.2 Microstructure After High Temperature Cyclic Tensile Test

Figures 9 and 10 show the grain distribution and grain boundary distribution of X70 pipeline steel after high-temperature cyclic tensile testing at different temperatures and strain rates. Comparing the grain distribution and grain boundary distribution before and after the test, the microstructure is polygonal ferrite. There are different degrees of

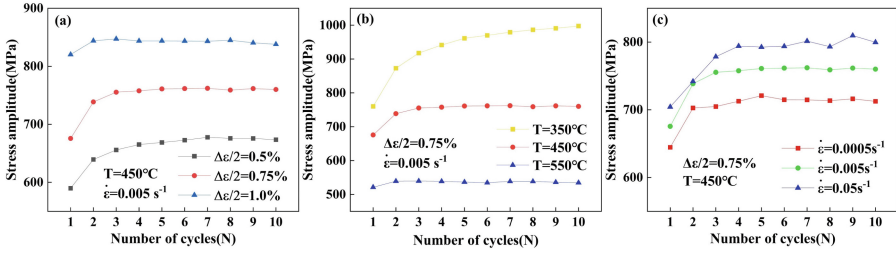


Fig. 8. Cyclic stress amplitudes for high-temperature cyclic tensile loads under different heat deformation conditions: (a) strain amplitude, (b) temperature, (c) strain rate.

black precipitates present under different hot deformation conditions in Fig. 9, which are mainly distributed inside the ferrite grains. These precipitates are attributed to the complex carbonitrides (Ti, Nb, V) (C, N), and their existence is closely related to the presence of fine grains and small-angle grain boundaries [11]. Additionally, by examining the grain size distribution and angular distribution of orientation difference in specimens before and after the test, as shown in Fig. 11, it is evident that high-temperature cyclic pulling within the temperature range of 350 °C to 550 °C and strain rate range of $0.0005s^{-1}$ to $0.05s^{-1}$ has a minimal effect on the microstructure changes of X70 pipeline steel.

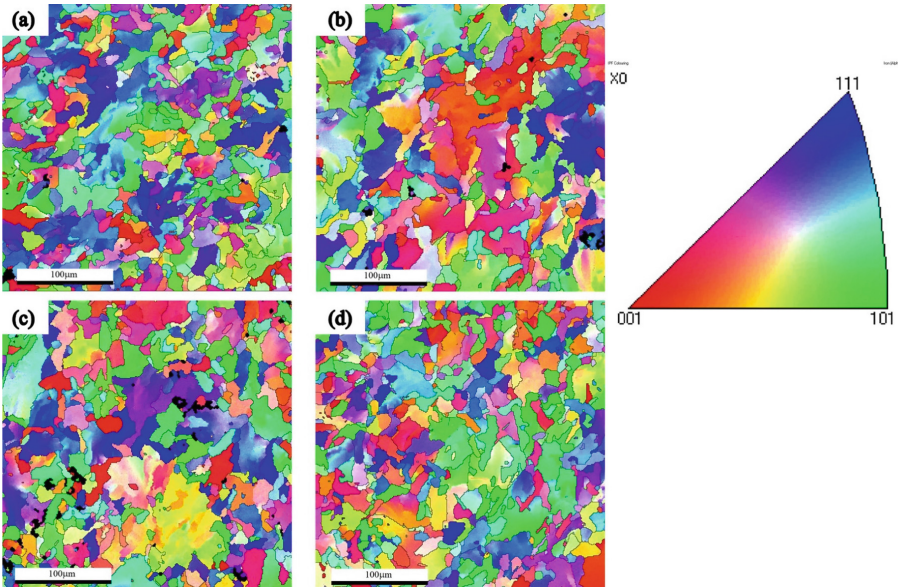


Fig. 9. Grain distribution under different heat deformation conditions: (a) $T = 350\text{ }^{\circ}\text{C}$, $\dot{\epsilon} = 0.05s^{-1}$, (b) $T = 550\text{ }^{\circ}\text{C}$, $\dot{\epsilon} = 0.05s^{-1}$, (c) $T = 350\text{ }^{\circ}\text{C}$, $\dot{\epsilon} = 0.0005s^{-1}$, (d) $T = 550\text{ }^{\circ}\text{C}$, $\dot{\epsilon} = 0.0005s^{-1}$.

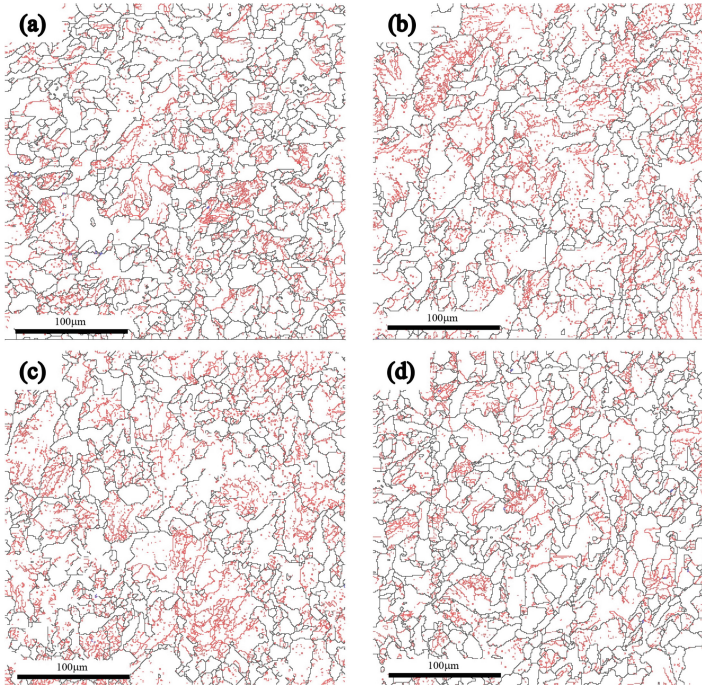


Fig. 10. Distribution of grain boundaries under different heat deformation conditions: (a) $T = 350^\circ\text{C}$, $\dot{\varepsilon} = 0.05\text{s}^{-1}$, (b) $T = 550^\circ\text{C}$, $\dot{\varepsilon} = 0.05\text{s}^{-1}$, (c) $T = 350^\circ\text{C}$, $\dot{\varepsilon} = 0.0005\text{s}^{-1}$, (d) $T = 550^\circ\text{C}$, $\dot{\varepsilon} = 0.0005\text{s}^{-1}$.

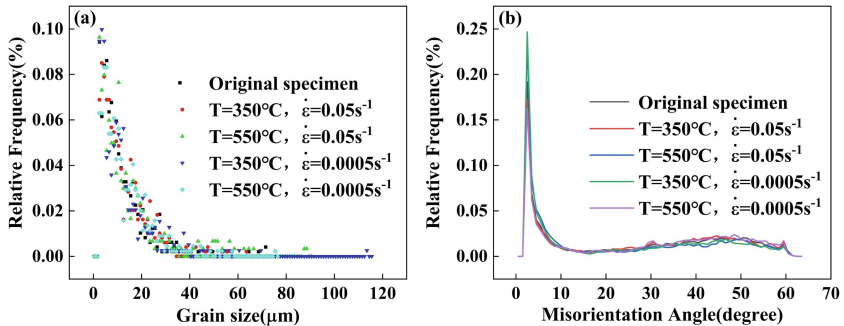


Fig. 11. Grain size and orientation difference angle distribution under different heat deformation conditions: (a) grain size, (b) orientation difference angle distribution.

4 Conclusions

- (1) In this paper, the cyclic hysteresis curves obtained from the high-temperature cyclic drawing and pressing experiments of X70 pipeline steel show that in the range of strain amplitude $\Delta\varepsilon/2 = 0.5\% \sim 1.0\%$, temperature $T = 350^\circ\text{C} - 550^\circ\text{C}$, strain rate $\dot{\varepsilon} = 0.0005\text{s}^{-1} \sim 0.05\text{s}^{-1}$, X70 pipeline steel shows certain rapid cyclic

hardening, the hardening rate gradually decreases, the strain amplitude and strain rate are related to The peak cyclic stress of X70 pipeline steel is positively correlated, and the temperature is negatively correlated with the peak cyclic stress of X70 pipeline steel.

- (2) In the range of strain amplitude $\Delta\varepsilon/2 = 0.5\%$ to 1.0% , temperature $T = 350\text{ }^{\circ}\text{C}$ to $550\text{ }^{\circ}\text{C}$, and strain rate $\dot{\varepsilon} = 0.0005\text{ s}^{-1}$ to 0.05 s^{-1} , the microstructure of X70 pipeline steel is minimally affected by high-temperature cyclic loading. This finding suggests that the thermal straightening process has little impact on the tissue properties of X70 pipeline steel under corresponding thermal deformation conditions.

References

1. Masoumi, M., Herculano, L.F.G., de Abreu, H.F.G.: Study of texture and microstructure evaluation of steel API 5L X70 under various thermomechanical cycles. *Mater. Sci. Eng. A* **639**, 550–558 (2015)
2. Kim, H.L., Park, S.H.: Loading direction dependence of yield-point phenomenon and bauschinger effect in API X70 steel sheet. *Metals Mater. Int.* **26**(1), 14–24 (2020)
3. Zhou, C.L., Xu, J., Wang, G.D., Liu, X.H.: Intermesh model of hot roller leveler for plate steel. *J. Iron Steel Res.* **18**(8), 28–31 (2006)
4. Wang, J.G., Chen, L., Li, T.Q., Li, G.: Controlling research of the pre-bending deformation before straightening and residual stresses after straightening for 100-meter. *Adv. Mater. Res.* **572**, 296–301 (2012)
5. Maksimov, E.A., Shatalov, R.L.: A study of the parameters for hot straightening of thick steel plates on a roller straightening machine. *Metallurgist* **62**(1–2), 132–137 (2018)
6. Seong, W.J., Na, S.J.: Systematization of heat straightening process of stiffened plate by surface flattening. *J. Mater. Process. Technol.* **299**, 117333 (2021)
7. Laugwitz, M., Jochum, M., Scheffer, T., Lohmar, J.: Towards hot levelling strategies for steel heavy plates: analysis of flatness evolution in accelerated cooling, hot level-ling, and final air cooling via thermo-mechanical FE modelling. *Int. J. Adv. Manuf. Technol.* **120**(3–4), 2469–2488 (2022)
8. Yu, Y., Wei, Y., Jinxing, J., Peng, L.: Yield stress of high-grade pipeline steel at high temperature and its effect on hot process. *Iron Steel* **48**(5), 46–50 (2013)
9. Zhou, C.L.: Simulation and mathematical model on hot plate roller levelling. Ph.D. thesis. Dissertation of Northeastern University, China (2006)
10. Yu, G.C., Zhao, J., Zhai, R.X., Wang, C.G.: Theoretical analysis and experimental investigations on the symmetrical three-roller setting round process. *Int. J. Adv. Manuf. Technol.* **94**, 45–56 (2018)
11. Wang, J., Atrens, A.: Microstructure and grain boundary microanalysis of X70 pipeline steel. *J. Mater. Sci.* **38**, 323–330 (2003)